ELSEVIER

Journal of Nuclear Materials 305 (2002) 1–7

journal of nuclear materials

www.elsevier.com/locate/jnucmat

The impact of irradiation temperature on the microstructure of F82H martensitic/ferritic steel irradiated in a proton and neutron mixed spectrum

X. Jia [a], Y. Dai [a,*], M. Victoria [b]

[a] *Spallation Source Division, Paul Scherrer Institut, CH-5232 Villigen PSI, Switzerland*
[b] *EPFL-CRPP-Fusion Technology Materials, 5232 Villigen PSI, Switzerland*

Received 20 February 2002; accepted 28 June 2002

Abstract

F82H low-activation martensitic steel was irradiated in the Swiss Spallation Neutron Source (SINQ) Target-III to irradiation doses of 10–12 dpa in a temperature range of 140–360 °C. Transmission electron microscope observations have been performed to study the radiation effects on the microstructure at different irradiation temperatures. The results show: (1) High-density helium bubbles of size $\geqslant 1$ nm are observed in the samples irradiated at temperatures $\geqslant 175$ °C. The size of bubbles increases with increasing irradiation temperature, but the density remains almost constant. (2) The irradiation temperature is the controlling parameter for the amorphization of the precipitates in F82H steel. Present work indicates that the amorphous temperature for typical precipitates ($M_{23}C_6$) is about 235 °C, corresponding to about $0.3T_m$ (T_m is the absolute melting point temperature) of the steel. (3) With increasing irradiation temperature, the mean size of the defect clusters remains almost constant below 235 °C, but increases rapidly at higher temperatures. The density of defect clusters shows no significant change up to 255 °C, and then decreases rapidly above this temperature.

1. Introduction

Due to its good thermal and mechanical properties, the low-activation ferritic/martensitic steel known as F82H is a candidate material for the first wall and blanket of the future fusion reactor [1]. It is also considered as a tentative candidate material for the container of the liquid target of the European spallation neutron source [2]. Because of these applications, irradiated ferritic/martensitic steels have been studied intensively in the last decades in an extensive irradiation temperature range (50–750 °C) and high irradiation doses (up to 200 dpa). However, the microstructure of ferritic/martensitic steels irradiated in the low temperature range (<350 °C) is not yet well understood.

The SINQ target irradiation program (STIP) was initiated in 1996 [3] under collaboration with ORNL, FZJ, JAERI, CEA, LANL and other laboratories. It is one of the key activities that aim at studying radiation damage in structural materials produced by high-energy protons plus spallation neutrons. The first program (STIP-I) was carried out in the SINQ Target-III from July 1998 to December 1999 with an interruption of three months at the beginning of 1999. A maximum dose of 12.5 dpa and helium concentrations of 900 appm were obtained in steel specimens. The irradiation temperature ranged from 90 to 370 °C. Different types of materials and specimens were positioned in rods placed at different positions of the target for irradiation. In particular, transmission electron microscope (TEM) samples of F82H steel were placed in four different rods at different

* Corresponding author. Tel.: +41-56 310 4171; fax: +41-56 310 2485/4529.
E-mail address: yong.dai@psi.ch (Y. Dai).

0022-3115/02/$ - see front matter
PII: S0022-3115(02)00916-9

positions, so a series of irradiation temperatures and doses were obtained for the TEM investigation. The present paper presents the results of the TEM investigation on the samples of 10–12 dpa.

2. Experimental

F82H steel (a 15 mm thick plate, IEA Heat 9741) used in this study was provided by the Fusion Technology Materials group (PIREX) of CRPP-EPFL, Switzerland. Its composition is: 7.65 Cr, 2 W, 0.16 Mn, 0.16 V, 0.02 Ta, 0.11 Si and 0.09 C in wt%, and Fe for the balance. The plate was subjected to a heat treatment: normalized at 1040 °C for 38 min and tempered at 750 °C for 1 h, which produces a fully martensite structure [4].

The TEM samples used in the present study were irradiated to 10–12 dpa. The irradiation was performed with a total proton current of about 0.85 mA for the first 12 months and about 1.04 mA for the last 2 months of the real beam time. The difference between the irradiation temperatures in these two periods is as high as 15% of the temperature values. The temperature values used in this report are the average of those in the two periods. More detailed information can be found in Ref. [3]. Table 1 summarizes the information on irradiation doses and temperatures of the samples.

The sample preparation is optimized in order to reduce magnetism and radioactivity using the following procedure. The normal 3 mm TEM samples were punched into 1 mm disks, which were then inserted into 1 mm holes punched into the center of 3 mm 304 stainless steel disks. The assembly was then glued with epoxy and ground from 250 μm thick down to about 150 μm before electro-polishing. Compared to that of original 3 mm TEM samples, the radioactivity was reduced by a factor of more than 10 after electro-polishing. Furthermore, the magnetic effects on TEM observation are also significantly reduced [5].

TEM investigation of the microstructure was performed at 200 kV on a JEOL 2010. The most often used image conditions were bright field (BF) and weak beam dark-field (WBDF) at $\mathbf{g}(4\mathbf{g})$, $\mathbf{g}(5\mathbf{g})$ and $\mathbf{g}(6\mathbf{g})$, $\mathbf{g} = 200$ near $\mathbf{z} = 011$. But only the micrographs of $\mathbf{g}(5\mathbf{g})$ were used for quantifying the size and density of defect clusters. A magnification of 150 000 or 200 000 times was used for the analysis of irradiation-induced defect clusters. For the observation of small helium bubbles a magnification of 250 000 times was often applied. Pictures of a final magnification 500 000–600 000 times were used for measuring the density and size of small clusters or helium bubbles. As the thickness of thin foils was deduced from the number of fringes, the uncertainty of the densities is estimated to be about ±15%.

3. Results

The microstructure of F82H prior to irradiation consisted of tempered-martensite laths. $M_{23}C_6$ type carbide precipitates were identified mainly along prior austenite grain boundaries and martensite lath boundaries. The size of precipitates varied from about 0.1 to 1 μm.

Fig. 1(a)–(e) shows the microstructure of F82H steel before and after irradiation. The tempered-martensite structure is stable after irradiation, even after the irradiation to a dose of 12.2 dpa at 360 °C (Fig. 1(b)). Size and distribution of carbides also show no distinct change after irradiation. However, the crystal structure of these precipitates can be changed significantly depending on the irradiation temperature. The present observations show that in the samples irradiated at and below 235 °C the precipitates have changed from the crystalline to the amorphous state after irradiation (Fig. 1(c)). There is a critical transition point from amorphous to crystalline at about 235 °C, as we can see from Fig. 1(d), part of the precipitates is transformed to amorphous but part of them still remains as crystalline. In the samples irradiated at above 235 °C, the precipitates remain crystalline after irradiation (Fig. 1(e)).

The irradiation-induced defect structure shows a strong dependence on irradiation temperature. Fig.

Table 1
F82H irradiation conditions and results of TEM measurements

Specimen	Dose (dpa)	Helium concentration (appm)	Irradiation temperature (°C)	Defect size (nm)	Defect density (m^{-3})	Bubble size (nm)	Bubble density (m^{-3})	Amorphization of carbides
P[17]	10.0	472	140 ± 13	3.7	3.60×10^{22}	–	–	Yes
RC6-05	10.2	480	175 ± 23	3.3	2.99×10^{22}	0.7	5.07×10^{23}	Yes
RC6-02	10.2	480	210 ± 29	3.5	3.44×10^{22}	0.8	4.58×10^{23}	Yes
RC6-01	10.2	480	235 ± 33	3.6	3.63×10^{22}	0.9	4.73×10^{23}	Partly
P[16]	10.3	490	255 ± 22	5.5	3.75×10^{22}	1.2	4.16×10^{23}	No
P[1]	9.9	470	295 ± 23	6.5	2.70×10^{22}	1.4	4.01×10^{23}	No
P[13]	12.2	818	360 ± 30	8.1	1.50×10^{22}	1.6	4.28×10^{23}	No

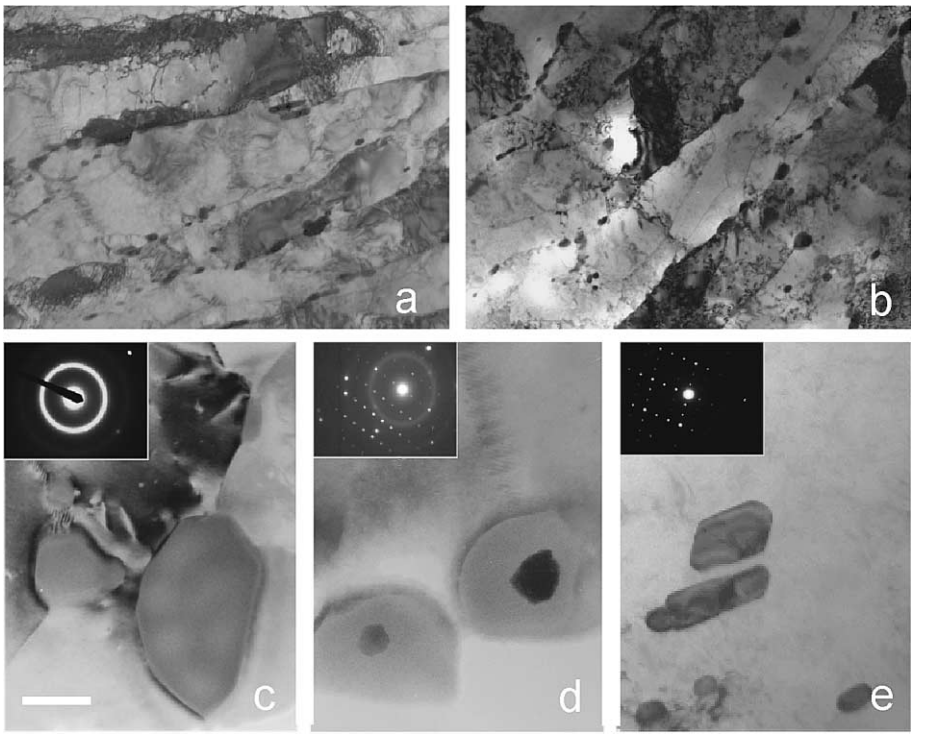

Fig. 1. The microstructure of F82H steel before and after irradiation: (a) unirradiated, (b) irradiated at 360 °C, 12.2 dpa, (c) irradiated at 210 °C, 10.2 dpa, (d) irradiated at 235 °C, 10.2 dpa and (e) irradiated at 255 °C, 10.3 dpa. The scale in the left corner of (c) represents 200 nm for (a), (b), 50 nm for (c), (d) and 100 nm for (e).

2(a)–(f) presents the microstructure in the samples irradiated at 140, 175, 210, 255, 295 and 360 °C to 10, 9.9, 10.2, 10.2, 10.3 and 12.2 dpa, respectively. The measured size and density of the defect clusters are presented in Table 1 and also plotted in Fig. 3. The data indicate that with increasing irradiation temperature, the density of defect clusters shows no significant change up to 255 °C, and then decreases rapidly above this temperature. The size of the defect clusters remains almost constant at temperatures below 235 °C, but increases rapidly at higher temperatures, which can be seen more clearly from the size distribution presented in Fig. 4.

The most interesting finding of the present work is that in the samples irradiated at about 175 °C and above, high-density helium bubbles with an average size around 1 nm were observed, as shown in Fig. 5(a)–(d) for different cases. The quantitative results of the size and density of the helium bubble distribution are presented in Table 1 and also plotted in Figs. 5 and 6. Obviously with increasing irradiation temperature from 175 to 360 °C the mean size of helium bubbles increases gradually from about 0.7 nm to about 1.6 nm while the density of helium bubbles decreases slightly from 5×10^{23} m^{-3} down to 4×10^{23} m^{-3}. No helium bubbles can be resolved in the samples irradiated at about 140 °C.

4. Discussion

The temperature dependence of the microstructure of the irradiated martensitic steels in the low temperature regime, namely $\leqslant 350$ °C, is not well understood. Although some work [5–10] has been performed, it is generally limited to one or two temperatures. A systematic study is needed to give a more complete picture. The present work has been performed for this purpose.

The general features of the microstructure in different types of martensitic steels irradiated at 300 °C and below observed by different researchers (e.g. [5–10]) are similar, namely the defect clusters (black dots) become identifiable at a low irradiation dose of less than 1 dpa. With increasing doses, the size and the number density increase. Although the dose dependence of the size and density of defect clusters has been studied, the irradiation temperature dependence is little known. From the present results it can be seen that in case of specimens irradiated to about 10 dpa, the density of defect clusters shows no significant changes up to 255 °C, and then decreases quickly at higher temperatures. The size of the defects clusters does not change much either with increasing temperature up to 235 °C, but increases rapidly above this temperature. Zinkle et al. reported that for irradiated copper, both the loop density and size

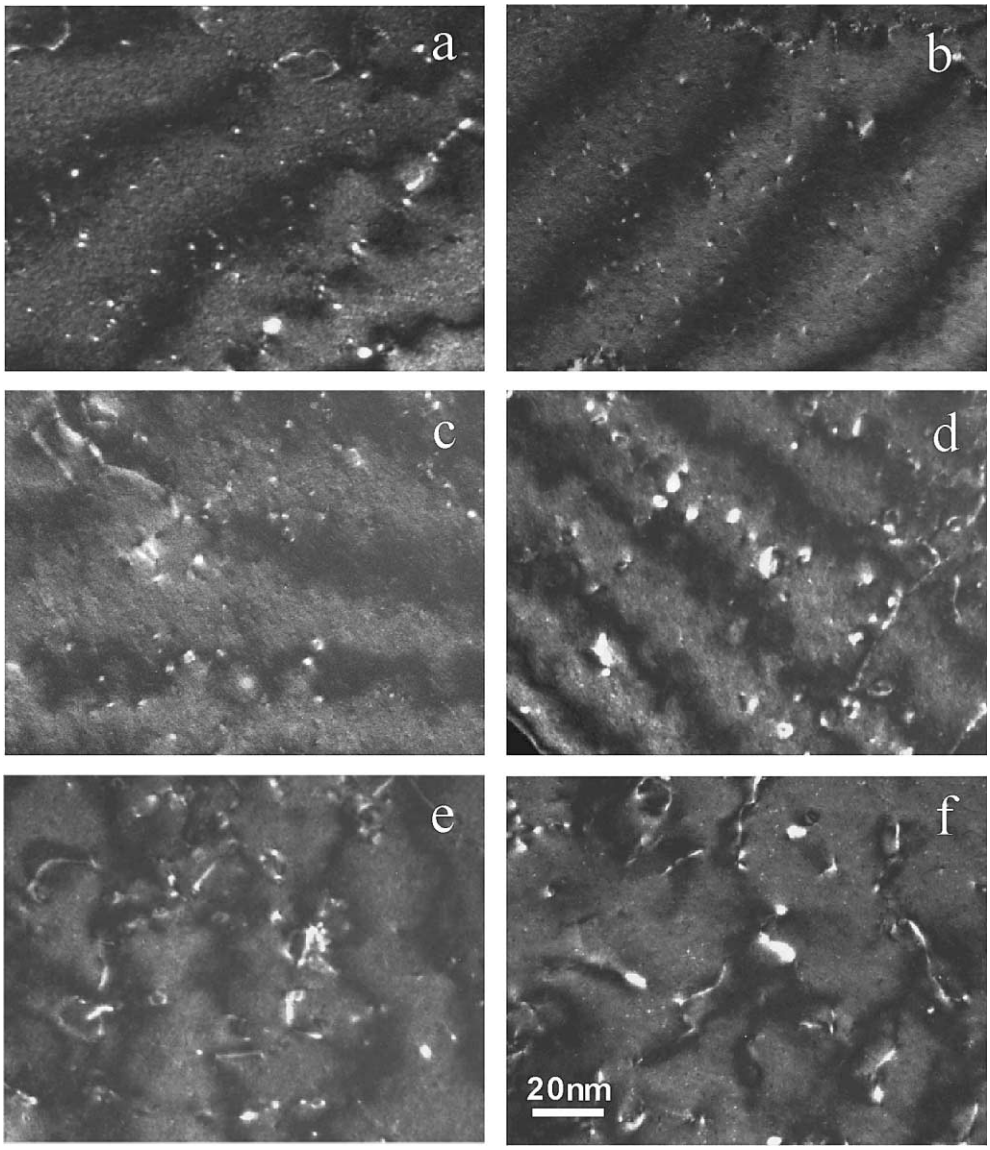

Fig. 2. Defect cluster structure for irradiated F82H steel: (a) 10.0 dpa/140 °C; (b) 10.2 dpa/175 °C; (c) 10.2 dpa/210 °C; (d) 10.3 dpa/255 °C; (e) 9.9 dpa/295 °C; (f) 12.2 dpa/360 °C.

decrease with increasing irradiation temperature between 60 and 200 °C, above 200 °C the density decreases and the size increases more quickly with increasing temperature [11]. This behavior is coherent with the present observations. At lower irradiation temperature, the build-up of irradiation-induced defects does not continue indefinitely. In this case the defect concentrations saturate as a result of spontaneous recombination processes from cascade overlaps. But with the increasing irradiation temperature, the defect clusters become more mobile and can either react with other defects of their native cascades or escape to different sinks. The recombination of interstitials and vacancies, as well as the growth and annihilation of dislocation loops cause the distinct drop of the defect cluster density.

The possibility of helium bubble nucleation in the regime $T < 0.3T_m$ has been the subject of discussion, particularly in terms of their possible effect on overall mechanical properties and the fracture behavior of the irradiated martensitic steels. Recently Singh et al. [12,13] studied neutron irradiated iron and copper using positron annihilation and electrical conductivity methods, showing that in iron, the defect structure in the as-irradiated state was dominated by microvoids during

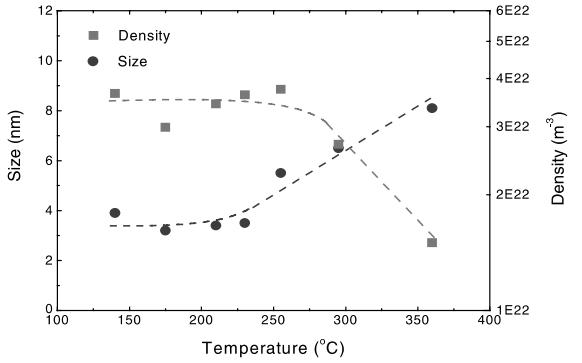

Fig. 3. Temperature dependence of the size and number density of defect clusters.

neutron irradiation at 100 °C, i.e. at a temperature between the annealing stage III and IV. With increasing annealing temperature from 100 to 250 °C, the density and the size of voids increased significantly, but in the temperature range 250–350 °C, i.e. in and above the annealing stage V, a coarsening of voids took place and the density decreased. The present observations demonstrate that, at this irradiation condition the lowest temperature for visible helium bubbles is around 175 °C. The helium bubbles are probably too small to be resolved in the samples irradiated at lower temperatures.

Generally helium bubbles are not readily observed with TEM after neutron or high-energy proton irradiation [5,7,8] at $\leqslant 250$ °C, although they were observed in steels after helium implantation at high temperatures (e.g. [14–16]). There are only few cases where helium bubbles or cavities were observed after neutron irradiation [10] or helium implantation [17] at 250 °C. In [10], helium bubbles were observed in martensitic steels OPTIFER-Ia, OPTIFER-II, F82H, ORNL-3791 (9Cr-2WVTa) and MANET-II irradiated in the HFR to 0.8 dpa. However, it is difficult to understand that the bubble density in OPTIFER-II (3.8×10^{24} m^{-3}) is two orders of magnitude higher than those in OPTIFER-Ia (1.5×10^{22} m^{-3}) and MANET-II (3.6×10^{22} m^{-3}) irradiated at the same condition, although the helium concentrations in these three steels are similar (60 appm for OPTIFER-Ia and OPTIFER-II, 70 appm for MANET-II). Furthermore, the bubble size of OPTIFER-II (3 nm) is even larger than those of OPTIFER-Ia (2 nm) and MANET-II (2 nm). In [17], small bubbles of 2–5 nm were observed in helium (400 appm) implanted F82H samples with TEM, which was also demonstrated by small angle neutron scattering (SANS) analysis. But there is no quantitative result of the helium bubble density. In martensitic steels irradiated with high-energy protons at temperatures $\leqslant 250$ °C, there are no helium bubbles or cavities observed perhaps due to either the low temperature [7,8] or low helium concentration [5]. The helium bubbles are believed too small to be observed with TEM.

The radiation-induced amorphization (RIA) is a rather complex phenomenon and at present is only qualitatively understood. Under low temperature irradiation, the RIA alloys, typically intermetallic compounds, first disorder and later, above a critical dose of

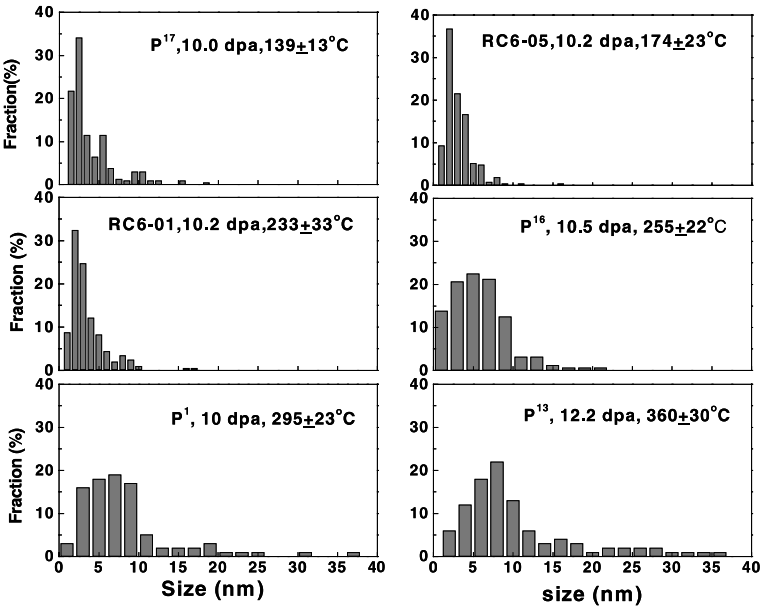

Fig. 4. The size distribution for defect clusters of the samples irradiated at different temperatures.

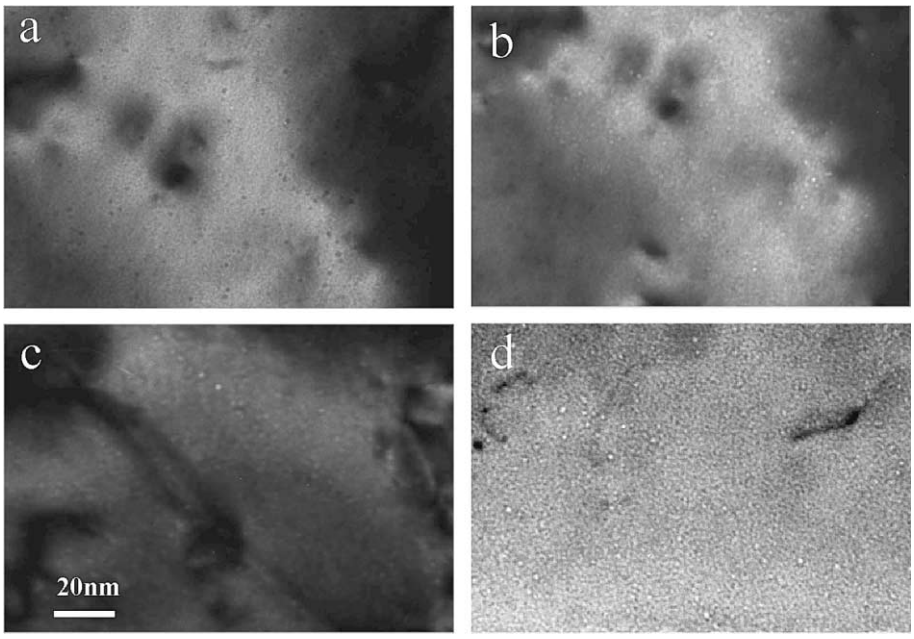

Fig. 5. High-density helium bubbles after irradiation at: (a) 10.3 dpa/255 °C, BF image and over-focused; (b) same condition as (a) but under-focused; (c) 9.9 dpa/295 °C; (d): 12.2 dpa/360 °C.

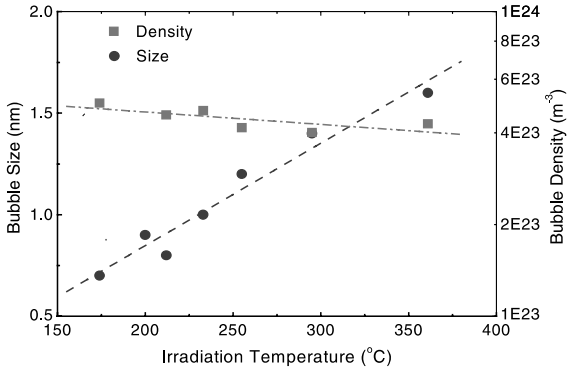

Fig. 6. The temperature dependence of sizes and densities of helium bubbles.

about 0.2–0.5 dpa, start to become amorphous [18]. This behavior can be interpreted by a destabilization of disordered zones through displacement cascade overlap, e.g. an existing disordered zone could be transformed later into the amorphous state by interstitial injection from nearby displacement cascades. Another possibility is that newly produced spike cores overlapping with existing disordered zones could remain amorphous if in the overlap region a different interfacial energy favors the amorphous over the disordered structure. At higher irradiation temperature, the radiation-induced point defects are mobile and try to restore the originally ordered structure. From the competition between the disordering effect of newly produced displacement cascades and the reordering effect of the mobile point defects, in RIA alloys, the mobile point defects can induce a transformation of the initially amorphous zones into crystalline zones. Therefore, a critical temperature, T_{AMO}, can be defined, above which a carbide precipitate can no longer be amorphized under irradiation. In the carbide precipitates (mainly $M_{23}C_6$) of F82H steel, the agglomeration and dissociation of C-vacancy clusters could play an important role in amorphization. The C-defect clusters are stable at temperatures up to 220–240 °C (e.g. stage IV), which may lead to extreme highly disordered (amorphized) precipitates. The observations of the present study and our previous work on irradiated martensitic steels [6–8] and austenitic steel SS304 [19] agree well with this hypothesis. Amorphization of the carbide precipitates has been observed by Dai et al. in several ferritic/martensitic steels [6–8] and in austenitic steel SS304 [19] after 800 MeV proton irradiation. The previous results show that the $M_{23}C_6$ precipitates have completely changed from crystalline to amorphous at a dose of about 2.3 dpa at irradiation temperatures lower than 230 °C. The series of results with irradiation temperature ranging from 140 to 360 °C in the present work show that at temperatures above 235 °C, the precipitates remain as crystalline while at temperatures below 235 °C they are amorphous. After irradiation at about 235 °C, part of the precipitates were transformed to amorphous

but part of them still remained as crystalline. This indicates that the critical temperature, T_{AMO}, is around 235 °C for the $M_{23}C_6$ precipitates.

5. Conclusion

Reduced activation ferritic martensitic steel F82H was irradiated in SINQ Target-III to 10–12 dpa in a temperature range of 140–360 °C. TEM observations have been conducted to investigate the impact of irradiation temperature on the microstructure. The results demonstrate:

1. High-density helium bubbles of about 1 nm diameter are observed in the samples irradiated at temperatures $\geqslant 175$ °C, the size of bubbles increases with increasing irradiation temperature, while the density decreases slightly.
2. With increasing irradiation temperature, the mean size of the defect clusters remains almost constant at temperatures below 235 °C, but increases rapidly at higher temperatures. The density of defect clusters shows no significant change up to 255 °C, and then decreases rapidly above this temperature.
3. The irradiation temperature is the controlling parameter for the amorphization of the precipitates in F82H steel. For F82H steel the amorphous temperature is about 235 °C, corresponding to about $0.3T_m$ (T_m is the absolute melting temperature) of the steel.
4. No irradiation-induced precipitates were found after irradiation to 12.2 dpa at 360 °C.

Acknowledgements

This work is included in both SPIRE (irradiation effects in martensitic steels under neutron and proton mixed spectrum) subprogram of the European 5th Framework Program and the ESS TMR program, which are supported by Swiss Bundesamt für Bildung und Wissenschaft. The authors would like to express thanks to Dr R. Schäublin for his help on TEM observation, Dr L.P. Ni for calculating the irradiation temperature, Mr K. Geissmann for his help on irradiation experiment.

References

[1] M. Tamura, H. Hayakasa, M. Tanimura, A. Hishinuma, T. Kondo, J. Nucl. Mater. 141–143 (1986) 1067.
[2] Y. Dai, in: Proceedings of the 13th Meeting of the Int. Collaboration on Advanced Neutron Sources (ICANS-XIII) and 4th Plenary Meeting of the European Spallation Source Project (ESS-PM4), 1995, p. 604.
[3] Y. Dai, G.S. Bauer, J. Nucl. Mater. 296 (2001) 43.
[4] Y. Kohno, D.S. Gelles, A. Kohyama, M. Tamura, A. Hishinuma, J. Nucl. Mater. 191–194 (1992) 868.
[5] R. Schaeublin, M. Victoria, J. Nucl. Mater. 283–287 (2000) 339.
[6] Y. Dai, G.S. Bauer, F. Carsughi, H. Ullmaier, S.A. Maloy, W.F. Sommer, J. Nucl. Mater. 265 (1999) 203.
[7] Y. Dai, F. Carsughi, W.F. Sommer, G.S. Bauer, H. Ullmaier, J. Nucl. Mater. 276 (2000) 289.
[8] Y. Dai, S.A. Maloy, G.S. Bauer, W.F. Sommer, J. Nucl. Mater. 283–287 (2000) 513.
[9] E. Wakai, N. Hashimoto, Y. Miwa, J.P. Robertson, R.L. Klueh, K. Shiba, S. Jistukawa, J. Nucl. Mater. 283–287 (2000) 799.
[10] E.I. Materna-Morris, M. Rieth, K. Ehrlich, in: M.L. Hamilton, A.S. Kumar, S.T. Rosinski, M.L. Grossbeck (Eds.), 19th International Symposium, ASTM STP, 1366, 2000, p. 597.
[11] S.J. Zinkle, A. Horsewell, B.N. Singh, W.F. Sommer, J. Nucl. Mater. 212–215 (1994) 132.
[12] M. Eldrup, B.N. Singh, J. Nucl. Mater. 276 (2000) 269.
[13] B.N. Singh, A. Horsewell, P. Toft, J. Nucl. Mater. 271–272 (1999) 97.
[14] H. Schroeder, P. Batfalsky, J. Nucl. Mater. 103&104 (1981) 839.
[15] W. Kesternich, Radiat. Eff. 78 (1983) 261.
[16] H. Henry, P. Jung, J. Chen, in press.
[17] R. Coppola, M. Magnani, R.P. May, A. Möslang, J. Appl. Cryst. 33 (2000) 469.
[18] W. Schilling, H. Ullmaier, in: R.W. Cahn, P. Haasen, E.J. Kramer (Eds.), Mater. Sci. Technol. 10b (1994) 179.
[19] Y. Dai, X. Jia, J. Chen, W.F. Sommer, M. Victoria, G.S. Bauer, J. Nucl. Mater. 296 (2001) 174.